CONF-850902--1

THE ROLE OF HYDROGEN EMBRITTLEMENT IN INTERGRANULAR STRESS CORROSION CRACKING OF SENSITIZED TYPE 304 STAINLESS STEEL*

W. E. RUTHER, T. F. KASSNER, AND F. A. NICHOLS

Materials Science and Technology Division
Argonne National Laboratory
Argonne, Illinois 60439

CONF-850902--1

TI85 014965

June 1985

DISCLAIMER

To be submitted for presentation at the Second Intl. Symp. on "Environmental Degradation of Materials in Nuclear Power Systems--Water Reactors," sponsored by ANS, Metallurgical Society of AIME, and NACE, September 9-12, 1985, Monterey, CA.

*Work supported by the Office of Nuclear Regulatory Research, U. S. Nuclear Regulatory Commission.

THE ROLE OF HYDROGEN EMBRITTLEMENT IN INTERGRANULAR STRESS CORROSION CRACKING OF SENSITIZED TYPE 304 STAINLESS STEEL*

W. E. RUTHER, T. F. KASSNER, AND F. A. NICHOLS
Materials Science and Technology Division
Argonne National Laboratory
Argonne, Illinois 60439
(312) 972-5191

ABSTRACT

Fixed-load Mode I/Mode III comparative tests have been conducted on lightly sensitized (EPR = 2 C/cm^2) Type 304 SS specimens in 289°C oxygenated water with other impurity additives. Substantial susceptibility to IGSCC was shown in Mode I but no conclusive evidence for SCC was found in Mode III. These results are consistent with a hydrogen embrittlement mechanism of crack advance, but electrochemical measurements seem to accord better with a slip-dissolution mechanism. Further studies are needed to clarify the operative mechanism(s).

INTRODUCTION

The two most-often cited processes for explaining the crack-advance during stress-corrosion cracking in aqueous solutions are slip-dissolution[1,2] and hydrogen-embrittlement.[3] In the former case, dissolution of the alloy at the crack tip, due to slip-induced cracking of a protective film, produces an increment of crack advance before repassivation stops the process. Thus, crack growth requires repeated ruptures by continuing plastic deformation of the alloy. Since the protective films are relatively impervious to hydrogen evolved from the cathodic reduction of hydrogen ions, hydrogen embrittlement also requires repeated film rupture, and therefore should not be considered an

*Work supported by the Office of Nuclear Regulatory Research, U. S. Nuclear Regulatory Commission.

alternative to the entire slip-dissolution model but an alternative only for the process of incremental crack advance.

Anodic dissolution at the crack tip is generally thought to obey Faraday's Law. The actual amount of dissolution can be related to the rate of film rupture which is relatively insensitive to the particular stress state (e.g., tension, shear). On the other hand, all available models for the embrittling effect of hydrogen presuppose the existence of a hydrostatic tensile stress near the crack tip.[4] Thus, stress states that have no hydrostatic component should not produce hydrogen embrittlement, whereas dissolution should proceed equally well with or without a hydrostatic stress provided fracture of the passive film at the crack tip occurs at approximately the same rate. Consequently, several investigators have suggested that the influence of loading mode may be a useful means of distinguishing hydrogen embrittlement from dissolution-related failure processes.

Stress corrosion cracking of α-brass in an ammoniated tarnishing solution[5] (6 g/ℓ of Cu powder dissolved in 14 N NH_4OH) occurs readily in both Mode I (tensile opening) and Mode III (pure shear). The former loading mode produces a large component of hydrostatic tension near the notch/crack tip whereas the latter produces none. This apparent insensitivity to loading mode implies that hydrogen embrittlement plays no significant role in the cracking process.

A number of investigators have shown that titanium-base alloys[5,6] and low-alloy martensitic[6] and 18Ni maraging[7] steels exhibit stress-corrosion cracking under Mode I loading in saline solutions (3.5% NaCl, acetic-acid and chromate-inhibited brines), trichloroethylene, and HCl/methanol environments but essentially no susceptibility in Mode III. This has been interpreted as

strong evidence for some type of hydrogen embrittlement process. Aluminum-base alloys[5,8-10] display an intermediate behavior with some susceptibility in Mode III but more in Mode I, which indicates partial roles for both dissolution and hydrogen embrittlement.

EXPERIMENTAL PROCEDURE

In view of the apparent success of Mode I/Mode III comparisons in elucidating the mechanism of crack advance at ambient temperatures, we have performed a series of comparative tests with both loading modes on sensitized Type 304 SS in 289°C water with ~7 ppm dissolved oxygen and several impurity species that are known to facilitate IGSCC in the material (e.g., oxyacids such as H_2SO_4 and H_3AsO_4).

A schematic of the loading system for the Mode I/Mode III tests is shown in Fig. 1. The top of the autoclave was fitted with either a tension or torsion loading system. The force due to the hydraulic pressure of the water on the feedthrough rod was considered in calculating the tensile load. In most of the Mode I tests, the constant tensile load was applied using Bellofram air cylinders with a regulated gas supply. In torsion testing, the force due to hydraulic pressure on the feedthrough rod was counteracted with a flat roller thrust bearing supported by the autoclave. Deadweight loads were converted to a constant torsional load by a flexible cable and ball-bearing pulley arrangement. The square-shank-ended torsion specimens were not restrained from movement in the axial direction.

Water is supplied to the 4-ℓ autoclave system via a regenerative heat exchanger and a small preheater at the autoclave inlet of the once-through water system. For most of the experiments, the electrochemical potentials of Type 304 SS and platinum electrodes located at the outlet of the autoclave

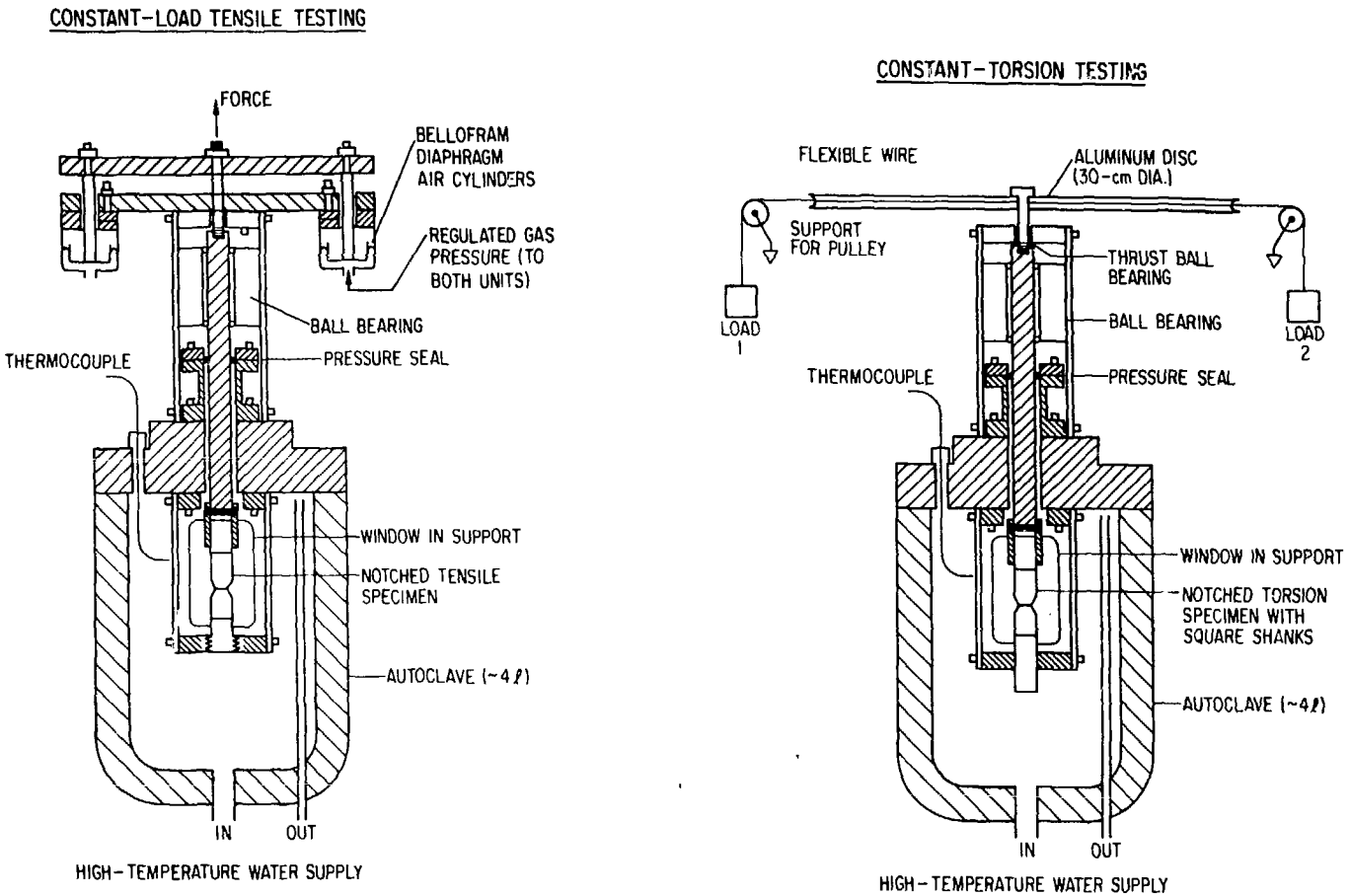

Fig. 1. Schematic of the (left) Tensile (Mode I) and (right) Torsion (Mode III) Loading Systems for SCC Experiments in High-Temperature Water.

were monitored relative to an external 0.1M KCl/AgCl/Ag reference electrode, and the values were converted to the standard hydrogen electrode at 289°C.

The specimens for both loading modes had circular cross sections of 11.1-mm diameter with 60° circumferential notches and a root radius of 0.1 mm, which produced a minimum load-bearing section 5.64-mm in diameter. Constant strain rate tests were conducted in air at 289°C to determine the maximum tensile, σ_m^t, and torsional, σ_m^s, strengths of the notched specimens. The maximum tensile and yield stresses were 654 and 340 MPa, respectively, where $\sigma_y^t = 0.52\ \sigma_m^t$. The values for the maximum torsional stress and the yield stress under torsional loading are 577 and 202 MPa, respectively, where $\sigma_y^s = 0.35\ \sigma_m^s$. The maximum torsional stresses reported in Table I were obtained from the relationship for elastic deformation of a cylinder, viz., $\sigma_m^s = 2T/\pi r_o^3$, where T is the torque applied to a specimen of radius r_o. For the case of large plastic yielding of the specimens, the maximum torsional stress can be obtained from the relation $\sigma_m^s = (3 + n)T/2\pi r_o^3$, where n is the work-hardening exponent ($n \sim 0.4$ for Type 304 SS). The torsional stress based on this equation is ~85% of the value obtained assuming elastic loading.

Several specimens were fatigue-precracked in air at ambient temperature, and the size of the remaining ligament was estimated by an ultrasonic technique. The ultrasonic measurements were calibrated with specimens containing EDM circumferential grooves and by fracturing the ligament of several precracked specimens in liquid nitrogen and measuring the depth of the fatigue cracks. As shown in Fig. 2, the fatigue precracks around the circumference of the specimen were of uniform depth.

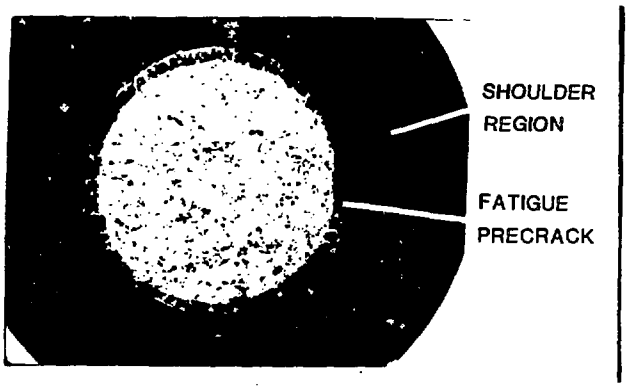

Fig. 2. Uniform Depth of a Fatigue Precrack at the Periphery of a Notched Torsion Specimen after Exposure to 289°C Water and Fracture at Liquid Nitrogen Temperature.

RESULTS

Results of SCC tests in 289°C water under Mode I and Mode III loading are summarized in Table I. Most of the experiments were performed in water with ~7 ppm dissolved oxygen and 0.1 ppm sulfate added as H_2SO_4. A few specimens were tested in water containing 0.25 ppm dissolved oxygen and 70 ppm $H_2AsO_3^-$; an environment that was found to be particularly deleterious in CERT experiments at 289°C and a strain rate of 1×10^{-6} s^{-1}. In all of the tests, the specimens were exposed to the environment for ~20 h at 289°C to form a corrosion film before loading in either tension or torsion.

The failure times are shown as a function of normalized stress, σ/σ_m, in Fig. 3 for the Mode I and Mode III experiments in oxygenated water with 0.1 ppm sulfate. The Mode I failure times range from several hours at a normalized stress level $\sigma/\sigma_m^t = 0.7$ to ~200 h at σ/σ_m^t of ~0.5. A typical intergranular fracture morphology is shown in Fig. 4.

TABLE 1. Stress Versus Time to Failure Results from Constant Tensile and Torsion Load Experiments on Sensitized (EPR = 2 C/cm^2) Type 304 SS Specimens[a] in 289°C Water with Different Impurity Species

	Feedwater Chemistry					Mode I/Mode III Loading Parameters							Potentials	
Test No.	Oxygen, ppm	Impurity Species	Anion Conc., ppm	Cond. at 25°C, μS/cm	pH at 25°C	Loading Mode	Maximum Stress, MPa	Fractional Stress, σ/σ_m	Failure Time, h	Reduction in Area, %	Angular Deflection, degrees	Fracture Morphology[b]	Type 304 SS, mV(SHE)	Pt, mV(SHE)
TE1	7.9	H_2SO_4	0.1	0.79	5.82	Tension	523	0.80	8.2	20	-	0.42D, 0.58I	180 ± 10	280 ± 10
TE6	7.0			0.91	5.76		425	0.65	1.6	7	-	0.34D, 0.66I		
TE2	7.8			0.75	5.87		392	0.60	6.6	8	-	0.28D, 0.72I		
TE7	7.1			0.85	5.77		379	0.58	90	6	-	0.30D, 0.70I		
TE8	6.6			0.90	5.76		360	0.55	116	6	-	0.25D, 0.75I		
TE5	7.7			0.92	5.71		360	0.55	>715[c]	-	-	-		
TE4	7.5			0.87	5.79		327	0.50	196	6	-	0.29D, 0.71I		
TE9	7.2			0.91	5.76		294	0.45	>2258[c]	-	-	-		
TE10	6.3			0.90	5.79		294	0.45	>235[c]	-	-	-		
TE3	7.3			0.84	5.78		262	0.40	>216[c]	-	-	-		
TO2	7.7			0.87	5.72	Torsion[d]	520	0.90	>794[c]	-	40	-		
TO6[e]	7.3			0.92	5.73		490	0.85[e]	>1149[c]	-	16	-		
TO1	7.9			0.88	5.75		462	0.80	>479[c]	-	20	-		
TO3[e]	5.4			0.90	5.75		462	0.80[e]	131	-	f	~1.00D		
TO5[e]	6.8			0.92	5.75		387	0.67[e]	>1011[c]	-	10	-		
TE11	0.25	H_3AsO_4[g]	70.0	410	3.07	Tension	523	0.80[h]	0.05	11	-	0.57D, 0.43I	460 ± 5	455 ± 5
TO8	0.25	H_3AsO_4[g]	70.0	410	3.05	Torsion[d]	462	0.80	>532[c]	-	20	-	460 ± 5	455 ± 5
TE12	7.1	$NaAsO_2$ / H_2SO_4	14.3 / 0.1	18.1	9.61	Tension	327	0.50	>1062[c]	-	-	-	135 ± 5	230 ± 5

[a]Specimens were exposed to the environment for ~20 h at 289°C before loading under tension or torsion.
[b]Ductile (D) and intergranular (I) in terms of the fraction of the cross-sectional area.
[c]Failure did not occur; the test was terminated at the indicated time.
[d]Maximum torsional stress was obtained from the relation for elastic loading: $\sigma_m^s = 2T/\pi r_o^3$, where T is the torque applied to the specimen of initial radius r_o. For large plastic yielding, the expression becomes $(3 + n)T/\pi r_o^3$, where n is the work-hardening exponent for stainless steel (~0.4). The maximum stress values are ~85% of those in the table.
[e]Specimens were fatigue-precracked; the fractional stress is based on ultrasound measurements of the uncracked area. Based on similar specimens, the fractional stress may be considerably higher.
[f]Not measured; the specimen failed in torsion.
[g]H_3AsO_4 master solutions were prepared by the oxidation of arsenic (III) oxide according to the reaction: $2As_2O_3 + 8HNO_3 + 2H_2O \rightarrow 4H_3AsO_4 + 8NO_2\uparrow$; consequently, the H_3AsO_4 solution may contain NO_3^- in addition to $H_2AsO_4^-$.
[h]This specimen was under a fractional stress σ/σ_m = 0.14 due to the autoclave pressure for ~20 h during the preloading period. Crack initiation and growth occurred during this period at the low stress level, and thus contributed to the short failure time at the higher stress level.

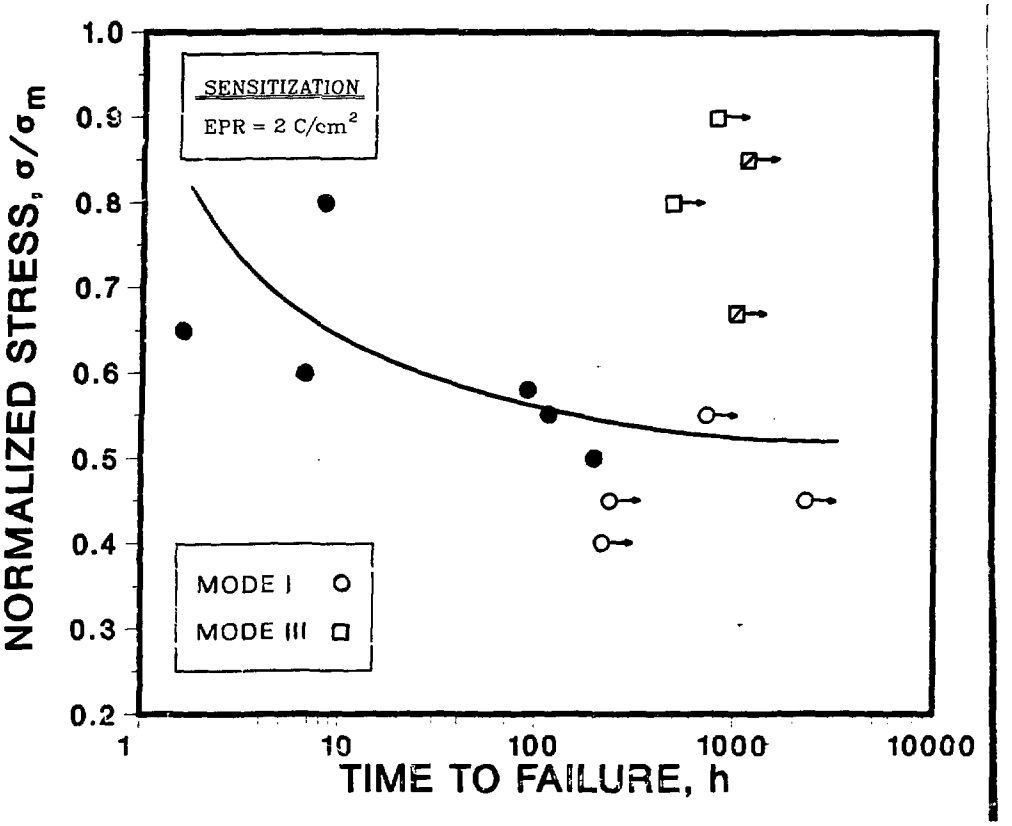

Fig. 3. Normalized Stress Versus Time to Failure of Lightly Sensitized (EPR = 2 C/cm^2) Type 304 SS Specimens in 289°C Water Containing ~7 ppm Dissolved Oxygen and 0.1 ppm Sulfate as H_2SO_4. Arrows signify that the test was terminated without failure at the indicated time; accented symbol ⧄ denotes a fatigue-precracked specimen.

Fig. 4. Typical Intergranular Fracture Morphology for a Lightly Sensitized (EPR = 2 C/cm^2) Type 304 SS Specimen under Mode I (Tensile) Loading in 289°C Oxygenated Water with 0.1 ppm Sulfate as H_2SO_4.

The Mode I test at a stress level of $\sigma/\sigma_m^t = 0.8$ in water containing 0.2 ppm dissolved oxygen and ~70 ppm $H_2AsO_3^-$ (Test No. TE-11 in Table I) failed essentially upon loading (~3 min); however, the specimen was under a normalized stress of $\sigma/\sigma_m^t = 0.14$ (due to the hydraulic pressure of water in the autoclave that acts on the feedthrough rod) for ~20 h during the preloading period. Examination of the fracture surface revealed numerous cracks of ~1.0 mm in depth with a dark corrosion product film that formed during this period. The reduced cross-sectional area no doubt contributed to the short failure time at the higher stress level.

In contrast to the high degree of IGSCC susceptibility of the material in the Mode I tests, no failures occurred in the notched specimens under Mode III loading at values of normalized stress σ/σ_m^s as high as 0.9 for time periods to ~1000 h. A specimen (Test No. T03 in Table I; not plotted) with a fatigue precrack, which could facilitate "initiation" of a stress corrosion crack as well as the development of the "crack-tip chemistry," failed in a ductile manner after ~130 h. Apparently, the fatigue precrack was deeper than the value determined from ultrasonic measurements, and the substantially higher stress, based on the reduced cross section, produced a creep-type failure in the material. The fracture surface in Fig. 5(a) shows virtually no corrosion during exposure in the autoclave. This is consistent with the predominantly ductile-dimple morphology in Fig. 5(b). A very small region of transgranular crack propagation adjacent to the fatigue precrack is evident in this micrograph, but no conclusive evidence for SCC was found in any of the Mode III specimens after fracture in liquid nitrogen.

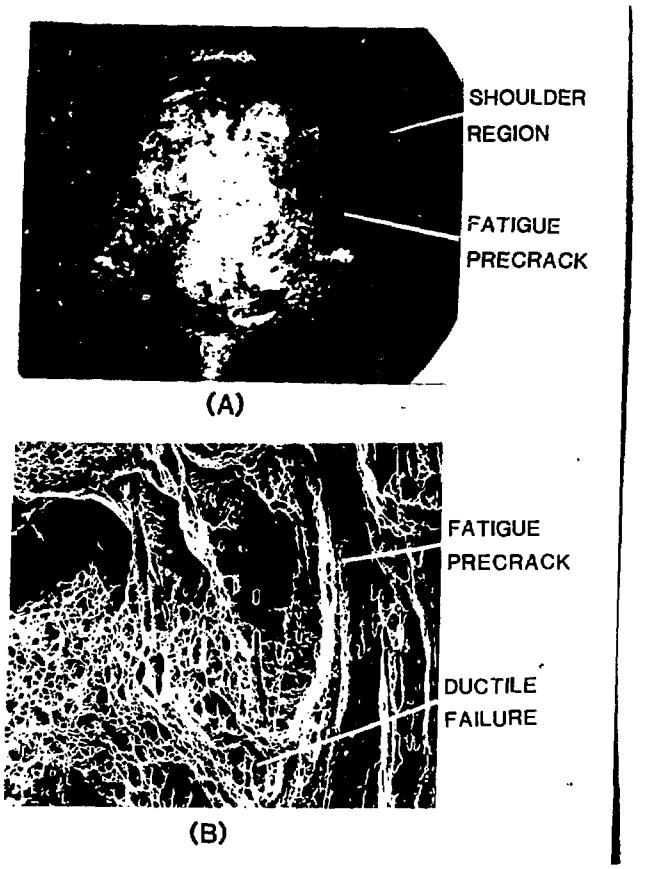

Fig. 5. Optical Micrograph of the Overall Fracture Surface of (a) a Fatigue-Precracked Torsion Specimen after a Failure in 289°C Water, and (b) an SEM Micrograph from the Periphery of the Specimen Showing the Ductile-Dimple Fracture Morphology.

DISCUSSION

The fact that SCC did not occur in either sharply notched or fatigue-precracked specimens of the lightly sensitized Type 304 SS under Mode III loading in aggressive environments for times much longer (factor of 10-100) than those required for failure under Mode I is in agreement with results obtained for the titanium-base alloys and high-strength steels in a variety of environments.[5-7] Similarly, the results are consistent with a hydrogen embrittlement mechanism of crack advance and do not appear to be in accord with the concepts of a dissolution mechanism.

Since crack initiation and growth did not occur under Mode III loading, any other evidence regarding the mechanism of crack advance must be derived

from Mode I loading experiments under constant load or constant strain-rate conditions. Information on the relative rates of different cathodic reactions, which are coupled with dissolution at the crack tip, as well as the influence of the two loading modes on the film-rupture process at the crack tip are of particular interest. Hydrogen ion reduction, with subsequent hydrogen absorption, is the predominant cathodic reduction process that occurs in the vicinity of the crack tip during hydrogen embrittlement. "Hydrogen entry catalysts," such as sodium arsenite at low temperatures, can act as hydrogen recombination inhibitors which retard the kinetics of hydrogen evolution and enhance hydrogen absorption and embrittlement. For example, the addition of 10 ppm As (as $NaAsO_2$) to salt solutions decreased the time to failure of titanium-[5] and aluminum-[9] base alloys under Mode I loading. Whether this arsenic species acts to enhance hydrogen uptake at the elevated temperatures employed here has not been established.

If the predominant cathodic reaction involved oxygen reduction ($O_2 + 2H_2O + 4e^- \rightarrow 4OH^-$) and/or the reduction of an oxyanion ($SO_4^{2-} + H_2O + 2e^- \rightarrow SO_3^{2-} + 2OH^-$ or $AsO_4^{3-} + 2H_2O + 2e^- \rightarrow AsO_2^- + 4OH^-$), stress corrosion cracking conceivably could proceed under Mode I loading without a significant contribution from hydrogen ion reduction. The experimentally determined dependence of the crack growth rate of Type 304 SS on the concentration of dissolved oxygen[11] as well as the dependence on the concentrations of H_2SO_4 and H_3AsO_4 in highly deoxygenated water (<5 ppb oxygen) at 289°C[12] strongly suggests that these cathodic reactions control the dissolution rate at the crack tip for a given strain rate or frequency of film rupture. In the absence of these species, i.e., low-oxygen, low-conductivity water, the susceptibility of the steel to IGSCC is mitigated significantly. Furthermore, sodium arsenite at concentrations greater than ~5 ppm of AsO_2^- completely inhibits IGSCC of sensitized Type 304 SS in CERT experiments in 289°C water

containing 0.2 ppm dissolved oxygen[12] (also see the Mode I results in Table I, Test Nos. TE-4 and -12). This is in contrast to its classical role as a hydrogen recombination inhibitor in ambient-temperature experiments where the time to failure of the specimens under Mode I loading is shorter in the presence of arsenic.[5,9] In our experiment, the $NaAsO_2$ species increases the $pH_{25°C}$ of the water from ~5.8 to 9.6 and conceivably retards the oxygen reduction reaction through the law of mass action in high-temperature water. Since arsenic in sodium arsenite is in the As^{3+} state, this species cannot itself participate in a reduction reaction that couples with anodic dissolution of the alloy crack tip.

Electrochemical potential measurements of stainless steel and platinum electrodes provide further insight into the rate-controlling electrode reactions in these environments. The open-circuit corrosion potentials of Type 304 SS in oxygenated water and in the arsenate (H_3AsO_4) solutions are quite anodic [+180 to 460 mV(SHE)] at 289°C, and thus the values are far removed from the negative potentials [-580 mV(SHE)] associated with hydrogen ion reduction at this temperature.[12] The corrosion potential approaches the latter value in low-oxygen, high-purity water where hydrogen ion reduction is the only viable cathodic reaction; however, under this condition, the steel is virtually immune to stress-corrosion cracking. Assuming the electrochemical potential at the tip of a crack or crevice is only slightly lower than at the specimen surface (i.e., the crack mouth) under open-circuit corrosion conditions,[13,14] the electrochemical measurements strongly imply that hydrogen ion reduction and the subsequent absorption of corrosion-product hydrogen are not major factors in SCC of sensitized Type 304 SS in high-temperature water.

It is difficult to reconcile the information pertaining to the role of dissolved oxygen and oxyanion impurity species on the crack growth rate of the steel in high-temperature water with the behavior in the Mode I/Mode III

tests. The reduction of these species at the crack mouth (external cathode) should occur equally well under both loading modes. Consequently, large differences in the SCC behavior of the steel for the two loading modes in the same environment may possibly be attributed to differences in the film-rupture or repassivation behavior. Since it is virtually impossible to initiate a crack during Mode III loading of Type 304 SS in the high-temperature aqueous environments, the rate of film rupture may be a more important factor than repassivation. The latter process could involve transport of dissolved oxygen and other species to the crack tip under conditions of minimal crack opening and thus would be important once crack growth begins.

With regard to the film rupture behavior at the root of the notched specimens, the actual stresses at the notch root, which control the strain rate and hence the film rupture rate, are not known precisely. In the elastic case, the stress concentration factor for the notch geometry under Mode III loading is approximately half of that under Mode I.[15] For small amounts of plastic yielding, the shapes of the plastic zone boundaries near the crack tip are also different for the two loading modes.[16] Although corresponding results for extensive plastic deformation are not available, the elastic and linear-elastic-fracture-mechanics cases suggest the possibility that the stress levels and deformation behavior at the notch root could be significantly different for the two loading modes (at the same fraction of the maximum loads). Creep rates in stainless steel (and hence the rupture rate of the oxide film) at the temperatures of interest (~150 to 300°C) are very sensitive to the stress level. For example, a recent model[17] suggests that the creep rate depends on the stress raised to the power r, where r is ~200. Thus, even small differences in the stress level for the two loading modes could have a large effect on the creep rate and consequently the film rupture process.

At high loads, i.e., fully plastic loading, the uniformity of the stress distribution across the specimen and the work-hardening behavior of the material are additional factors that may influence the film rupture behavior under the two loading modes. In the tensile mode, the stress is uniformly distributed across the specimen. Any deformation (by creep) at the surface is easily accommodated by deformation within the interior of the specimen, since every element or region is under the same stress. However, in the torsion mode, the stress is not uniformly distributed across the specimen. Hence, even if the stress levels at the surface are comparable in the two cases, the deformation at the surface of the torsion specimen is restrained by the inner region of material under lower stress. For a perfectly plastic material, i.e., an alloy that exhibits very little work hardening, the shear stress is uniformly distributed across the specimen, and a load controlled tension-torsion comparison may be valid. However, for a strongly work-hardening material such as stainless steel, the comparison becomes more complex. Although this could possibly account for the lack of susceptibility in Mode III, the argument should apply equally well to α-brass, also a strongly work-hardening material but one which shows strong susceptibility in Mode III.

Based on all of our results pertaining to the SCC behavior of the steel, it is difficult to conclusively rule out the hydrogen embrittlement mode of crack advance in the material, but, in view of the contrary electrochemical measurements, further studies are indicated.

REFERENCES

1. F. P. FORD, "Stress Corrosion Cracking," in Corrosion Processes, R. N. Parkins, ed., Applied Science Publishers, New York, pp. 271-309 (1982).

2. D. A. VERMILYEA, in Proc. Intl. Conf. on Stress Corrosion Cracking and Hydrogen Embrittlement of Iron Base Alloys, R. W. Staehle, J. Hochmann, R. D. McCright, and J. E. Slater, eds. NACE, Houston (1983), p. 208.

3. W. W. GERBERICH and Y. T. CHEN, Met. Trans. 6A, 271-278 (1971).

4. C. St. JOHN and W. W. GERBERICH, Met. Trans. 4, 589-594 (1973).

5. J. A. S. GREEN, H. W. HAYDEN, and W. C. MONTAGUE, in Effect of Hydrogen on Behavior of Materials, A. W. Thompson and I. M. Bernstein eds., TMS-AIME, New York (1976), p. 200.

6. C. F. ST. JOHN, Scripta Met. 9, 141-144 (1974).

7. H. W. HAYDEN and S. FLOREEN, Corrosion 27, 429-433 (1971).

8. J. R. PICKENS, J. R. GORDON, and L. CHRISTODOULOU, in High-Strength Powder Metallurgy Aluminum Alloys, M. J. Koczak and G. J. Hildemon eds., AIME (1982), pp. 177-192.

9. J. R. PICKENS, J. R. GORDON, and J. A. S. GREEN, Met. Trans. 14A, 925-930 (1983).

10. M. P. MUELLER, A. W. THOMPSON, and I. M. BERNSTEIN, Corrosion 41(3), 127-136 (1985).

11. W. E. RUTHER, W. K. SOPPET, and T. F. KASSNER, in Materials Science and Technology Division Light-Water-Reactor Safety Research Program: Quarterly Progress Report, NUREG/CR-3689 Vol. IV, ANL-83-85 Vol. IV, October-December 1983 (August 1984), pp. 57-75.

12. W. E. RUTHER, W. K. SOPPET, and T. F. KASSNER, in Light-Water-Reactor Safety Materials Engineering Research Programs: Quarterly Progress Report, October-December 1984, NUREG/CR-3998 Vol. III, ANL-84-60 Vol. III, to be published.

13. G. J. BIGNOLD, Corrosion 28(8), 307-312 (1972).

14. P. DOIG and P. E. J. FLEWITT, in Mechanisms of Environment Sensitive Cracking of Materials, The Metals Society, London (1977), pp. 113-124.

15. R. E. PETERSON, Stress Concentration Factors, J. Wiley, New York, 1974.

16. D. BROCK, Elementary Engineering Fracture Mechanics, Third Edition, M. Nijhoff Publishers, 1982, pp. 98-99.

17. A. K. MILLER and T. TANAKA, in Development of an Engineering Model for Predicting IGSCC Damage, EPRI NP-2808-LD, Electric Power Research Institute, Palo Alto, February 1983.